

# Integrated proteomic analysis of tumor necrosis factor $\alpha$ and interleukin $1\beta$ -induced endothelial inflammation

Eelke P. Béguin<sup>a</sup>, Bart L. van den Eshof<sup>a</sup>, Arie J. Hoogendijk<sup>a</sup>, Benjamin Nota<sup>b</sup>, Koen Mertens<sup>a,c</sup>, Alexander B. Meijer<sup>a,d</sup>, Maartje van den Biggelaar<sup>a,\*</sup>

<sup>a</sup> Department of Molecular and Cellular Hemostasis, Sanquin Research, Amsterdam 1066 CX, the Netherlands

<sup>b</sup> Department of Research Facilities, Sanquin Research and Landsteiner Laboratory, Amsterdam Medical Center, University of Amsterdam, Amsterdam 1066 CX, the Netherlands

<sup>c</sup> Department of Pharmaceutics, Utrecht Institute for Pharmaceutical Sciences (UIPS), Utrecht University, Utrecht 3584 CS, the Netherlands

<sup>d</sup> Department of Biomolecular Mass Spectrometry and Proteomics, Utrecht Institute for Pharmaceutical Sciences (UIPS), Utrecht University, Utrecht 3584 CS, the Netherlands

## ARTICLE INFO

### Keywords:

Endothelium  
Inflammation  
TNF $\alpha$   
IL-1 $\beta$   
Proteomics  
Phosphoproteomics  
Cell surface proteomics

## ABSTRACT

The vascular endothelium provides a unique interaction plane for plasma proteins and leukocytes in inflammation. The pro-inflammatory cytokines Tumor Necrosis Factor  $\alpha$  (TNF $\alpha$ ) and interleukin  $1\beta$  (IL-1 $\beta$ ) have a profound effect on endothelial cells, which includes increased levels of adhesion molecules and a disrupted barrier function. To assess the endothelial response to these cytokines at the protein level, we evaluated changes in the whole proteome, cell surface proteome and phosphoproteome after 24 h of cytokine treatment. The effects of TNF $\alpha$  and IL-1 $\beta$  on endothelial cells were strikingly similar and included changes in proteins not previously associated with endothelial inflammation. Temporal profiling revealed time-dependent proteomic changes, including a limited number of early responsive proteins such as adhesion receptors ICAM1 and SELE. In addition, this approach uncovered a greater number of late responsive proteins, including proteins related to self-antigen peptide presentation, and a transient increase in ferritin. Peptide-based cell surface proteomics revealed extensive changes at the cell surface, which were in agreement with the whole proteome. In addition, site-specific changes within ITGA5 and ICAM1 were detected. Combined, our integrated proteomic data provide detailed information on endothelial inflammation, emphasize the role of the extracellular matrix therein, and include potential targets for therapeutic intervention.

**Significance:** Pro-inflammatory cytokines induce the expression of cell adhesion molecules in vascular endothelial cells. These molecules mediate the adhesion and migration of immune cells across the vessel wall, which is a key process to resolve infections in the underlying tissue. Dysregulation of endothelial inflammation can contribute to vascular diseases and the vascular endothelium is therefore an attractive target to control inflammation. Current strategies targeting endothelial adhesion molecules, including PECAM, CD99, ICAM1 and VCAM1 do not completely prevent transmigration. To identify additional therapeutic targets, we mapped the endothelial proteome after pro-inflammatory cytokine treatment. In addition to the whole proteome, we assessed the surface proteome to focus on cell adhesion molecules, and the phosphoproteome to uncover protein activation states. Here, we present an integrated overview of affected processes which further improves our understanding of endothelial inflammation and may eventually aid in therapeutic intervention of imbalanced inflammation.

## 1. Introduction

Acute inflammation is part of the body's immune response aimed to

protect against damage caused by for instance pathogens, trauma or toxins. Activation of innate and adaptive immune cells, by recognition of pathogen-associated molecular patterns or specific antigens, induces

**Abbreviations:** TNF $\alpha$ , Tumor Necrosis Factor  $\alpha$ ; IL-1 $\beta$ , interleukin  $1\beta$ ; NF $\kappa$ B, Nuclear Factor Kappa-light-chain-enhancer of activated B cells; AP1, Activator Protein 1; ICAM1, Intercellular Adhesion Molecule 1; VCAM1, Vascular Cell Adhesion Molecule 1; SELE, E-Selectin; BOEC, Blood Outgrowth Endothelial Cell; SILAC, Stable Isotope Labeling with Amino acids in Cell culture; TEER, Transendothelial Electrical Resistance

\* Corresponding author at: Plesmanlaan 125, 1066 CX Amsterdam, the Netherlands.

E-mail address: [m.vandenbiggelaar@sanquin.nl](mailto:m.vandenbiggelaar@sanquin.nl) (M. van den Biggelaar).

<https://doi.org/10.1016/j.jprot.2018.08.011>

Received 12 June 2018; Received in revised form 15 August 2018; Accepted 23 August 2018

Available online 25 August 2018

1874-3919/ © 2018 Elsevier B.V. All rights reserved.

the release of a variety of biochemical factors, including chemokines and cytokines. These affect the local environment, ultimately resulting in an increased blood flow, promotion of leakage of plasma-protein-rich fluid and localized recruitment and activation of circulating leukocytes [1]. Under normal conditions, the acute inflammatory response is quickly dampened upon removal of the stimulus. However, failure to regulate or resolve the inflammatory process can result in chronic inflammation, which can contribute to various diseases, including inflammatory bowel disease and rheumatoid arthritis [2–4]. Most research in the field of inflammation has focused on the role of innate and adaptive immune cells. However, endothelial cells (ECs) also play an important role in inflammation due to their strategic position lining the vasculature. This position on the border of blood and tissue allows ECs to facilitate the extravasation of circulating immune cells into the inflamed tissue [1,5] and may therefore represent an attractive target for therapeutic intervention. However, our insight in the molecular wiring of inflamed ECs is currently limited.

The endothelium responds to a variety of inflammatory cytokines and chemokines, produced by leukocytes, macrophages, platelets, vascular smooth muscle cells and by ECs themselves [6]. Most studies have focused on two pro-inflammatory cytokines: tumor necrosis factor (TNF) $\alpha$  and interleukin (IL)-1 $\beta$ . Using classical biochemical techniques, it has been well established that inflammatory activation of ECs results in an increased expression of adhesion molecules such as E-selectin (SELE) [7], vascular cell adhesion molecule-1 (VCAM1) [8], and intercellular adhesion molecule-1 (ICAM1) [7]. More recently, mass spectrometry-based approaches have been employed to study cytokine-induced signaling pathways in numerous cell types [9], including ECs [10,11]. These have facilitated the simultaneous quantification of thousands of proteins, and thereby considerably improved our understanding of the complex pathways of pro-inflammatory cytokine activation. It is now well established that TNF $\alpha$  and IL-1 $\beta$  binding to their respective receptors, TNF Receptor 1 (TNFR1) and IL-1 Receptor 1 (IL-1R1), results in recruitment of a signaling complex that activates a set of mitogen-activated protein kinase kinase kinases (MAPKKKs) [12,13]. These subsequently initiate signaling cascades that lead to the activation of the transcription factors NF $\kappa$ B (nuclear factor kappa-light-chain-enhancer of activated B cells) and Activator protein 1 (AP1, also known as JUN) resulting in increased expression of pro-inflammatory molecules, including adhesion molecules ICAM1, VCAM1 and SELE, chemokines and enzymes, as well as the reorganization of the actin cytoskeleton [14,15].

However, despite this progress, proteomic studies generally lack spatial and temporal resolution [9]. This is highly relevant, since continuous treatment with TNF $\alpha$  and IL-1 $\beta$  results in an apparent time-dependent protein expression profile. This is illustrated by protein levels of SELE, VCAM1 and ICAM1 [16,17]. At first SELE expression is drastically increased, which is followed by expression of VCAM1 and ICAM1 [16,17]. Yet, despite the continuous presence of cytokines, the increased proteins levels of SELE do not persist: within 24 h, the abundance of SELE starts to decline [16,17]. This suggests that regulatory mechanisms are in place that control protein levels in a time-dependent fashion, and raises the question how levels of other proteins develop over time. In addition, blocking antibodies against the adhesion molecules ICAM1, VCAM1, PECAM1 or CD99 do not completely prevent leukocyte extravasation [18–23], spurring a renewed interest in the quantification of other cell surface receptors under inflammatory conditions. Lastly, the similarities and differences between the effects of TNF $\alpha$  and IL-1 $\beta$ -treatment on endothelial cells are unclear [24].

Here, we addressed these questions by combining global proteome profiling with quantitative peptide-based cell surface proteomics and phosphoproteomics of prolonged TNF $\alpha$  and IL-1 $\beta$ -induced inflammation. Furthermore, we assessed protein levels over time in order to evaluate their kinetic profiles. Our integrated analysis identifies various novel cytokine-responsive proteins and provides insight into regulation of cytokine-responsive processes and pathways.

## 2. Materials and methods

### 2.1. Cell culture

Blood outgrowth endothelial cells (BOECs) were isolated and cultured as previously described [25]. BOECs derived from 3 healthy donors were pooled and used for ECIS, immunofluorescence, and mass spectrometry experiments.

### 2.2. Electric Cell-substrate Impedance Sensing (ECIS)

BOECs were grown to confluency on ECIS Cultureware 8W10E PC 8 well clusters (Applied Biophysics) treated for 15 min with 10  $\mu$ M L-cysteine (Sigma-Aldrich) and coated with 50  $\mu$ g/ml collagen type I (BD Biosciences). Experiments were performed in three independent replicates on an ECIS Z0 Array station at 32000 Hz. Cells were stimulated by adding IL-1 $\beta$  or TNF $\alpha$  (Peprotech) to a final concentration of 10 ng/ml, or thrombin at a final concentration of 10 nM. Resistance values were normalized to the time point before stimulation.

### 2.3. Immunofluorescence imaging

BOECs were grown on collagen-coated coverslips until confluent. Cells were stimulated with fresh pre-warmed EBM medium (Lonza), supplemented with SingleQuots (Lonza) and containing 18% FCS (Bodinco), and supplemented with IL-1 $\beta$ , TNF $\alpha$  or mock treated as described above. Cells were washed three times with wash buffer (10 mM HEPES, 135 mM NaCl, 10 mM KCl, 5 mM CaCl $_2$ ·2 H $_2$ O, 2 mM MgSO $_4$ ·7 H $_2$ O, pH 7.5), fixed in 4% (v/v) paraformaldehyde (Electron Microscopy Sciences) in wash buffer for 15 min and quenched by incubating 15 min in 50 mM NH $_4$ Cl in wash buffer. Samples were washed three times with phosphate buffered saline (PBS) (Fresenius Kabi), incubated for 10 min in blocking/permeabilization buffer (1% (w/v) bovine serum albumin (Merck), 0.1% (v/v) saponin in PBS), incubated 1 h with primary antibodies (mouse  $\alpha$ ICAM1 BBA3 (R&D Systems), goat  $\alpha$ hVE-Cadherin sc-6458 (Santa Cruz Biotechnology)) in blocking buffer, washed three times with PBS, incubated 1 h with secondary antibodies (chicken anti mouse IgG AlexaFluor (AF)488, Donkey anti Goat IgG AF568 (both ThermoFisher Scientific), CF633-labeled phalloidin (Biotium)) in blocking buffer, washed 3 times with PBS and once with demineralized water, and mounted in Prolong Gold Antifade Mountant (ThermoFisher Scientific). Samples were imaged on a LSM510/meta confocal scanning microscope system equipped with a 63 $\times$  Plan-Apochromat 1.40 oil immersion objective (Carl Zeiss MicroImaging).

### 2.4. SILAC cell culture

For mass spectrometry analysis, BOECs were grown in SILAC (Stable Isotope Labeling with Amino acids in Cell culture) EBM-2 medium (without Arginine and Lysine, custom made, Lonza), EGM-2 bulletkit (Lonza) and supplemented with 20% FCS (Bodinco) during passage 1–3 and 20% 1 kDa MWCO-filter in-house dialyzed FCS for passage 4 and 5. The cultures were SILAC-labeled by supplying isotope-labeled Arginine and Lysine residues in a ‘light’ (Arg0, Lys0) (Sigma-Aldrich), ‘medium’ (Arg6, Lys4) and ‘heavy’ (Arg10, Lys8) (Cambridge Isotopes) variant [26]. Cultures were passaged 5 $\times$  to ensure > 95% incorporation of labeled amino acids in the proteomes. Samples were prepared in triplicate with SILAC label switching. SILAC BOECs were grown to confluency and mock-, IL-1 $\beta$  or TNF $\alpha$  (10 ng/ml) treated for 24 h.

### 2.5. Cell surface labeling

SILAC-labeled cells were washed with wash buffer (10 mM HEPES, 135 mM NaCl, 10 mM KCl, 5 mM CaCl $_2$ ·2 H $_2$ O, 2 mM MgSO $_4$ ·7 H $_2$ O, pH 7.5) and labeled with 3 mM EZ-link Sulfo-NHS-LC-Biotin (Thermo Scientific) in wash buffer, for 30 min at 4  $^{\circ}$ C. The label was quenched by

washing four times with 100 mM Glycine in wash buffer.

## 2.6. Mass spectrometry sample preparation

Cells were lysed in 4% SDS, 100 mM DTT, 100 mM Tris, pH 7.5, supplemented with HALT phosphatase and protease inhibitor cocktail (Thermo Scientific). Light, medium and heavy SILAC-labeled samples were combined in a 1:1:1 protein ratio and subjected to Filter-Aided Sample Preparation (FASP) as described by Wiśniewski et al. [27]. For whole proteome analysis tryptic peptides were desalted using C18 StageTips [28]. In-depth whole proteomes were obtained by fractionation of 50 µg tryptic peptides using Strong Anion eXchange (SAX) using Empore Anion and Cation Exchange-SR Extraction Disks (3M) as described by Wisniewski et al. [27], with elution buffers of pH 11, 8, 6, 5, 4 and 3. The flow-through was acidified with TFA and loaded onto a separate C18 StageTip. For cell surface proteome analysis, the remaining tryptic digests were vacuum dried, supplemented with NaCl to a final concentration of 150 mM with a volume of 450 µl. The samples were divided over 3 wells of a SigmaScreen Streptavidin coated 96-wells cluster (Sigma-Aldrich), which was prewashed three times with wash buffer (50 mM NH<sub>4</sub>HCO<sub>3</sub>, 150 mM NaCl, pH 8.3). After overnight incubation at 4 °C, the unbound fraction was transferred and subjected to another round of streptavidin pull-down and wells were washed 5 times with wash buffer. Biotinylated peptides were subsequently eluted with 50 µl 5% formic acid, 70% acetonitrile (ACN) per well for 2 h at 4 °C followed by a second elution for 5 min at 4 °C with the same elution buffer. Eluates from the same sample and the same round of pull-down (in total 300 µl) were pooled, vacuum dried to 20 µl, diluted to 100 µl with 0.5% acetic acid, acidified to pH < 2.5 with trifluoroacetic acid (TFA) and desalted using C18 StageTips. For phosphoproteomic analysis, samples were processed as previously described [29]. Briefly, phosphopeptides were enriched using Phos-TiO beads (GL Sciences), after which the eluted peptides were desalted using C18 StageTips.

## 2.7. Mass spectrometry analysis

Tryptic peptides were separated by nanoscale C18 reverse chromatography coupled on line to an Orbitrap Fusion Tribrid mass spectrometer (Thermo Scientific) via a nanoelectrospray ion source (Nanospray Flex Ion Source, Thermo Scientific). Peptides were loaded on a 20 cm 75–360 µm inner-outer diameter fused silica emitter (New Objective) packed in-house with ReproSil-Pur C18-AQ, 1.9 µm resin (Dr Maisch GmbH). The column was installed on a Dionex Ultimate3000 RSLC nanoSystem (Thermo Scientific) using a MicroTee union formatted for 360 µm outer diameter columns (IDEX) and a liquid junction. The spray voltage was set to 2.15 kV. Buffer A was composed of 0.5% acetic acid and buffer B of 0.5% acetic acid, 80% acetonitrile. Peptides were loaded for 17 min at 300 nl/min at 5% buffer B, equilibrated for 5 min at 5% buffer B (17–22 min) and eluted by increasing buffer B from 5 to 15% (22–87 min) and 15–38% (87–147 min), followed by a 10 min wash to 90% and a 5 min regeneration to 5%. For whole proteome and cell surface proteome samples, analysis was performed as described before [30]. Briefly, survey scans of peptide precursors from 400 to 1500 *m/z* were performed at 120 K resolution (at 200 *m/z*) with a  $1.5 \times 10^5$  ion count target. Tandem mass spectrometry was performed by isolation with the quadrupole with isolation window 1.6, HCD fragmentation with normalized collision energy of 30, and rapid scan mass spectrometry analysis in the ion trap. The MS<sup>2</sup> ion count target was set to 10<sup>4</sup> and the max injection time was 35 ms. Only those precursors with charge state 2–7 were sampled for MS<sup>2</sup>. The dynamic exclusion duration was set to 60 s with a 10 ppm tolerance around the selected precursor and its isotopes. Monoisotopic precursor selection was turned on. The instrument was run in top speed mode with 3 s cycles. For phosphoproteome samples a slightly adjusted protocol was used: the resolution of the survey scan was set to 240 K with a  $2 \times 10^5$  ion count target. Tandem mass spectrometry was performed on

the 10 most intense ions by isolation using the quadrupole and analysis in the Orbitrap at a resolution of 30 K. The MS<sup>2</sup> ion count target was set to  $5 \times 10^4$  with a maximum injection time of 60 ms. All data were acquired with Xcalibur software.

## 2.8. Proteome data processing and analysis

Raw files were analyzed with the MaxQuant (1.5.3.8) computational platform [31]. Proteins and peptides were identified using the Andromeda search engine by querying the human Uniprot database (release 2–2015, 89,796 entries) using standard settings. Relative quantification was based on SILAC (Arg0Lys0, Arg6Lys4 and Arg10Lys8) using unique peptides for quantification only and enabling the ‘re-quantify’ and ‘match between runs’ options. To prevent bias from SILAC labeling, labels were switched for replicates. Log<sub>2</sub> SILAC ratios are reported. For the cell surface proteome the addition of a biotin group (339.16166 Da) was used as a variable modification and for the phosphoproteome ‘Phospho (STY)’ was used as a variable modification. Two subsequent pull-downs of biotin- and phosphopeptides of the same sample were treated as fractions of the same sample. MaxQuant output tables were loaded and analyzed using Rstudio 1.0.44 using R version 3.3.2. [32]. In brief, ‘reverse’, ‘potential contaminant’, ‘only identified by site’ and peptides quantified in < 3 replicates in 1 condition were filtered out. For phosphoproteomic analysis only class I phosphopeptides [33] were selected (localization probability > .75, score difference > 5). For cell surface proteome analysis biotinylated peptides were filtered according to the same criteria. Statistical analysis was performed using a linear model without intercept and applying contrasts for each comparison in cases with multiple comparisons. For data containing a single experimental group, one-sample *t*-tests were performed. *P* values were adjusted for multiple testing using Benjamini-Hochberg and *p* < .05 and a log<sub>2</sub> fold change ≥ 1 was considered significant and relevant. Results were imported in Perseus (1.5.3.2) software to generate heat-plots. For Gene Ontology-term enrichment analysis, gene lists of significantly affected proteins/peptides were generated. For cell surface proteome enrichment, GO-term enrichment of biotin-modified peptides compared to the whole peptide pool was assessed using Cytoscape 3.4.0. [34] with the BiNGO plug-in [35]. Ontology and annotation datasets were downloaded on 3-3-2016 from the Gene Ontology Consortium website ([www.geneontology.org](http://www.geneontology.org)). Enrichment analysis of stimulus-affected proteins was performed using the hypergeometric method from goseq [36] (1.24.0), FDR adjusted *p*-values < .05 were considered significant. The significantly enriched GO-terms were grouped and visualized with gogadget [37] (2.0), using hierarchical clustering of the overlap indexes (with ward.D agglomeration method and Euclidean distance). Similarity between the GO-terms was further visualized in networks with Cytoscape's Enrichment Map [38] plugin. The PhosphoPath plug-in [39] was employed to visualize affected proteins. The .raw MS files and search/identification files obtained with MaxQuant have been deposited in the ProteomeXchange Consortium (<http://proteomecentral.proteomexchange.org/cgi/GetDataset>) via the PRIDE partner repository [40] with the dataset identifier PXD009174.

## 3. Results

### 3.1. TNFα and IL-1β induce ICAM1 expression and decrease barrier function in primary endothelial cells

Our mass spectrometry-based protein quantification relies on the metabolic incorporation of stable isotope-labeled amino acids in cell culture (SILAC). For accurate protein quantification, this incorporation should exceed 95%, which is typically achieved after 5 cell passages. Blood outgrowth endothelial cells (BOECs) were used in this study for their superior propagation capacity [25]. To study endothelial inflammation, BOECs were treated with TNFα or IL-1β.

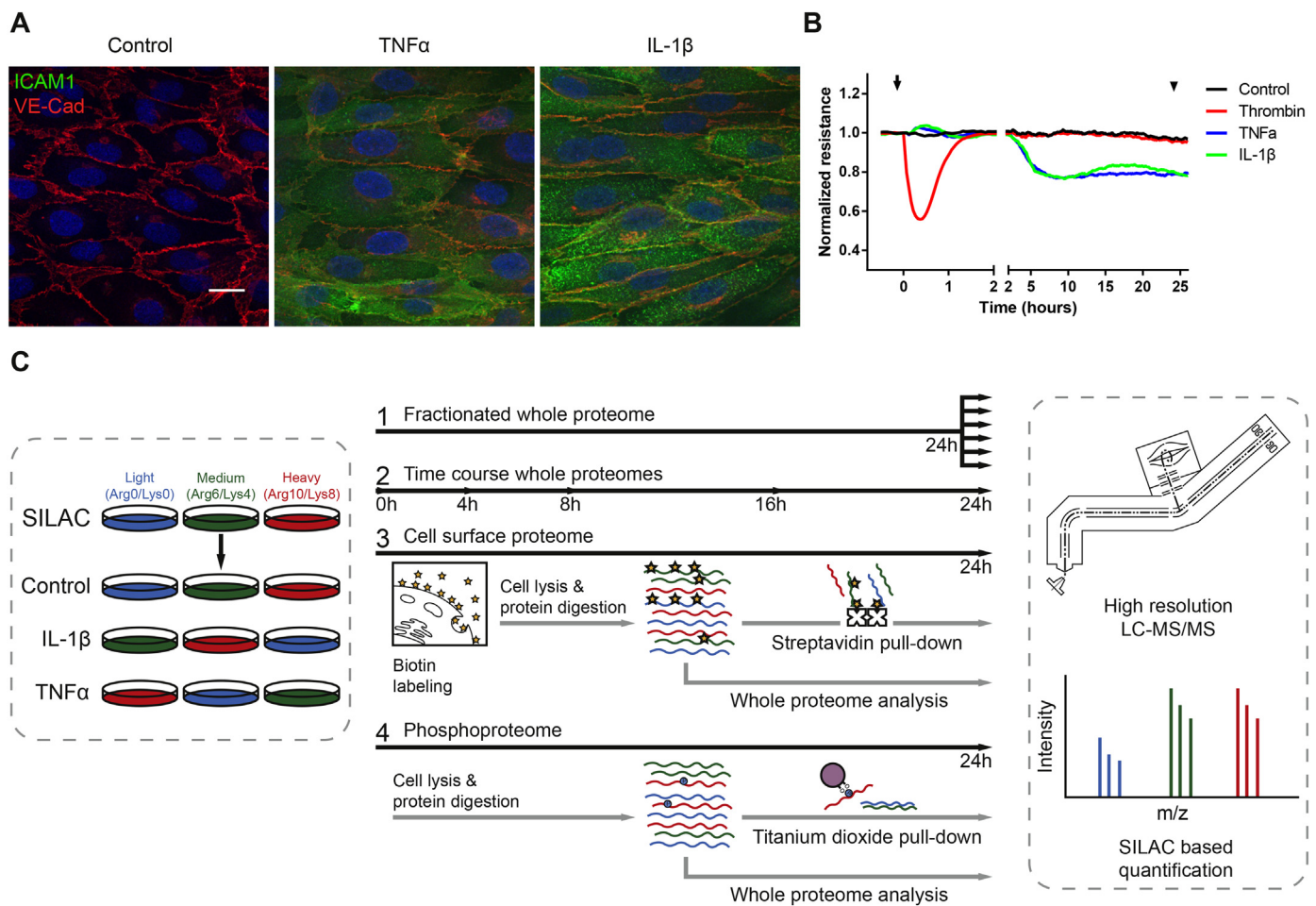


**Fig. 1.** Endothelial cells respond strongly to pro-inflammatory cytokines and proteomic workflow. (A) Immunofluorescence micrographs of BOECs treated with 10 ng/ml IL-1 $\beta$  or TNF $\alpha$  for 24 h. Green represents ICAM1, red VE-cadherin and blue is DAPI. The scale bar is 20  $\mu$ m. (B) Transendothelial electrical resistance of BOECs treated with 10 nM thrombin, TNF $\alpha$  or IL-1 $\beta$  (both 10 ng/ml), assessed by ECIS. Depicted are mean values of 6 replicates. The arrow indicates the moment of treatment, the arrowhead the time-point of proteomics read-out. (C) Proteomics workflow. SILAC-labeled BOECs are treated with 10 ng/ml TNF $\alpha$  or IL-1 $\beta$  for 24 h, either or not labeled with a non-membrane-permeable biotin label and combined in a 1:1:1 protein ratio. Proteins are digested into peptides by trypsin using FASP and tryptic digests are directly subjected to high resolution LC-MS/MS. In parallel, biotinylated peptides are pulled-down via streptavidin-coated plates or phosphopeptides are pulled-down using phospho-TiO beads. Subsequently, samples are subjected to LC-MS/MS analysis.

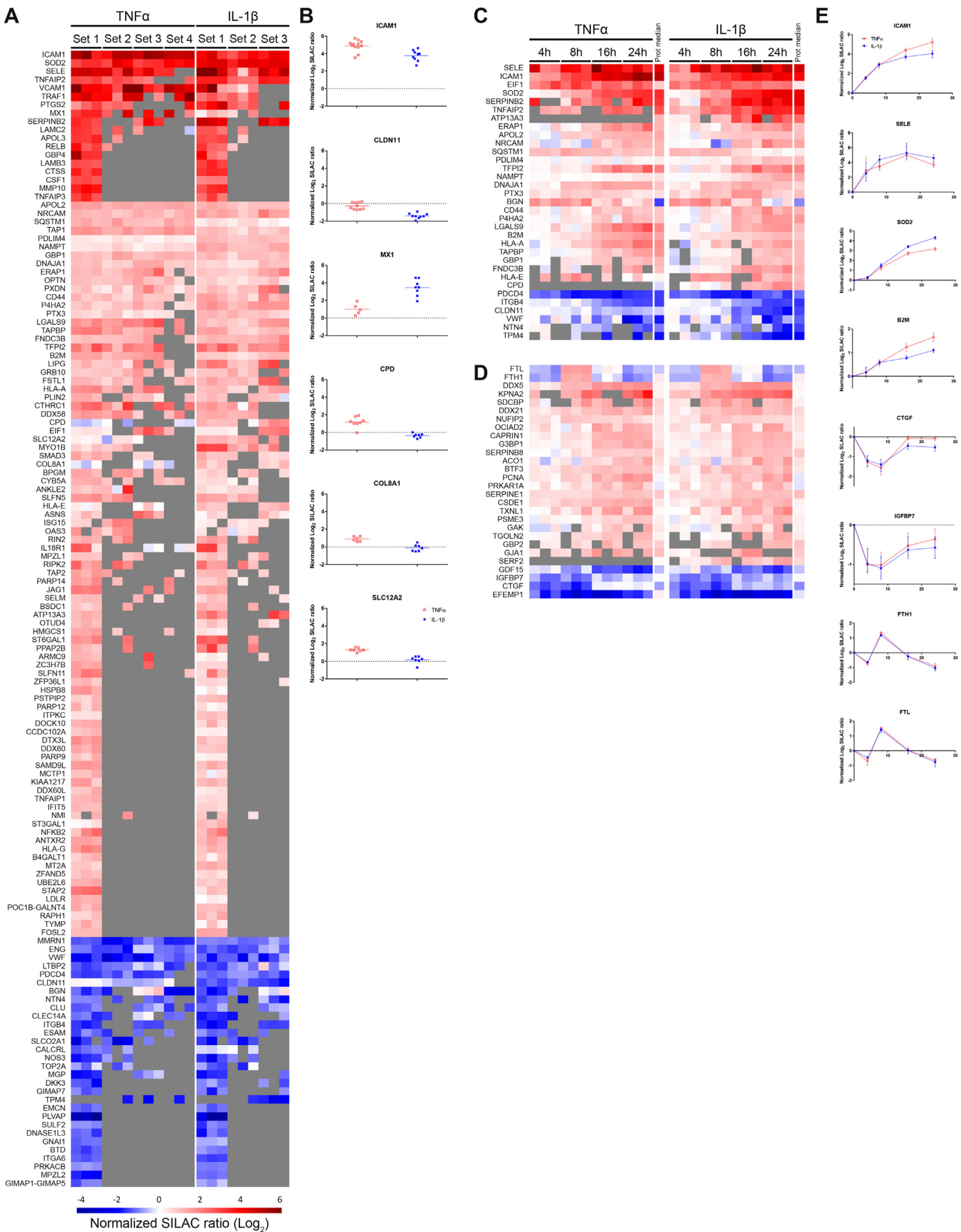
Immunofluorescence imaging confirmed that ICAM1 expression was drastically increased in cytokine-treated cells, yet a high degree of heterogeneity between cells was observed (Fig. 1A). Pro-inflammatory cytokine treatment reduces the endothelial barrier function [41]. To determine the duration of the cellular response, we assessed the endothelial barrier function in time using the transendothelial electrical resistance (TEER). In contrast to the rapid decrease (< 30 min) of TEER induced by thrombin, an enzyme of crucial importance in hemostasis [42], TNF $\alpha$  and IL-1 $\beta$  induced a delayed decrease in TEER similar in both extent and duration (Fig. 1B). After 2 h of cytokine treatment, the TEER gradually decreased to a steady-state, which was reached after about 7.5 h and continued for the duration of the stimulus. Combined, these two hallmarks of endothelial inflammation, increased expression levels of ICAM1 at the cell surface and the decreased endothelial barrier function, confirm the effectiveness of our cytokine-treatment.

### 3.2. TNF $\alpha$ and IL-1 $\beta$ provoke a comparable proteomic profile in ECs with specific fine-tuning

To gain insight into the effect of cytokine-induced signaling on protein levels, we performed proteomic analyses on cytokine- and mock-treated cells. Four experiments were performed, each consisting of a SILAC triplicate: 1) whole proteome (fractionated to improve

depth), 2) whole proteome time-course, 3) cell surface proteome, 4) phosphoproteome (Fig. 1C). For the cell surface proteome and the phosphoproteome, the whole proteome was assessed as well. In these four whole proteome datasets, 4596 proteins were quantified of which 136 were significantly affected after 24 h of TNF $\alpha$  or IL-1 $\beta$  treatment (Fig. 2A). The majority of the affected proteins (106) showed an increased protein profile. Interestingly, TNF $\alpha$  and IL-1 $\beta$  induced a highly similar response. Our quantitative mass spectrometry-based approach enabled us to estimate the relative protein quantities. Although this revealed subtle differences in protein levels, TNF $\alpha$  and IL-1 $\beta$  treatment resulted in very similar protein profiles. Only five proteins were significantly different between these cytokines: CLDN11 (claudin 11), MX1 (Interferon-induced GTP-binding protein Mx1), CPD (Carboxypeptidase D), COL8A1 (collagen alpha-1(VIII) chain) and SLC12A2 (solute carrier family 12 member 2) (Fig. 2B). As expected, for both cytokines, the most prominently affected proteins were adhesion receptors ICAM1, VCAM1 and SELE [7,8], which were on average 20 to 32 fold increased in TNF $\alpha$ -treated cells, followed by other known TNF $\alpha$ -responsive proteins including SOD2 (superoxide dismutase 2), TRAF1 (TNF receptor associated factor 1) and MX1 [43–45], which were on average between 12 and 22 fold increased (Fig. 2A, Table S1). In addition to these well-known proteins [7,8], we identified upregulation of a variety of proteins that have not been previously associated





(caption on next page)

**Fig. 2.** TNF $\alpha$  and IL-1 $\beta$  provoke a similar time-dependent proteomic signature with specific fine-tuning. Heat maps of proteins affected by treatment with either TNF $\alpha$  or IL-1 $\beta$  (10 ng/ml). Color coding represents log2 SILAC ratios, grey values were not quantified. (A) Of the 4596 quantified proteins, 136 were significantly affected in either of the treatment conditions. The heat map represents data after 24 h cytokine treatment obtained from 4 independent experiments: a fractionated whole proteome (set 1), cell surface labeling experiments (set 2, see also Fig. 3), the time-course experiment (set 3, see also panel c) and the phosphoproteome data (set 4, see also Fig. 4). (B) Proteins differentially affected by TNF $\alpha$ - and IL-1 $\beta$  treatment, and as a reference ICAM1. (C) Affected proteins identified in a time course experiment, which were also significant in the whole proteomes after 24 h. (D) Affected proteins identified in a time course experiment which did not correspond with the whole proteomes. (E) Time curves of selected proteins. Mean values and ranges of individual values are plotted for each condition. See also Table S-1.

with endothelial inflammation, such as TFPI2 (tissue factor pathway inhibitor 2), BPGM (bisphosphoglycerate mutase) and FNDC3B (fibronectin type III domain containing 3B) (Fig. 2A). In contrast, a number of proteins showed a decreased expression profile (Fig. 2A). These data are in agreement with previous observations that expression of NOS3 (nitric oxide synthase 3) is decreased under inflammatory conditions [46] and that secretion of VWF (von Willebrand Factor) is increased [47]. In addition to these, the abundance of other unknown cytokine-responsive proteins were lower in treatment conditions, including the extracellular matrix protein LTBP2 (latent transforming growth factor beta binding protein 2), membrane proteins ENG (endoglin), ESAM (endothelial cell adhesion molecule) and ITGB4 (integrin beta 4), and secreted proteins MMRN1 (multimerin 1) and NTN4 (netrin 4) (Fig. 2B). Interestingly, PLVAP (plasmalemma vesicle associated protein), which forms a physical sieve that regulates lymphocytes transmigration and plasma protein leakage [48,49], was also decreased (Fig. 2B).

### 3.3. Pro-inflammatory cytokines induce early and late-responsive proteins

To understand the temporal regulation of the induced response and to gain further insight in the dynamics of regulated proteins, we performed a longitudinal time-series by assessing protein levels after 4, 8, 16 and 24 h of cytokine-treatment. In agreement with a rapid onset of action, already after 4 h of treatment several proteins showed increased expression, including the leukocyte-interactors SELE and ICAM1. Consistent with previous reports [16,17], ICAM1 levels were still increasing after 24 h, whereas SELE levels were peaked well before 24 h of stimulation (Fig. 2C,E). Likewise, other proteins, including serine protease inhibitor B2 (SERPINB2), and sequestosome 1 (SQSTM1), a scaffold protein involved in NF $\kappa$ B signaling, were rapidly elevated within the first 4 h of treatment (Fig. 2C). In contrast, the abundance of other proteins, including PDCD4 (programmed cell death 4) and IGFBP7 (insulin-like growth factor binding protein 7), were decreased after 4 h of treatment (Figs. 2C and D). However, most regulated proteins were stable before 8 or 16 h of treatment, indicating the presence of a limited initial protein response, supporting leukocyte interaction, and a later extensive inflammatory response. Interestingly, a subset of proteins was transiently affected (Fig. 2E): a transient peak in ferritin levels (FTL [ferritin light chain] and FTH1 [ferritin heavy chain 1]) and a transient dip in CTGF (connective tissue growth factor) and IGFBP7 levels was observed after 8 h, after which these proteins returned to basal levels (Fig. 2C and E).

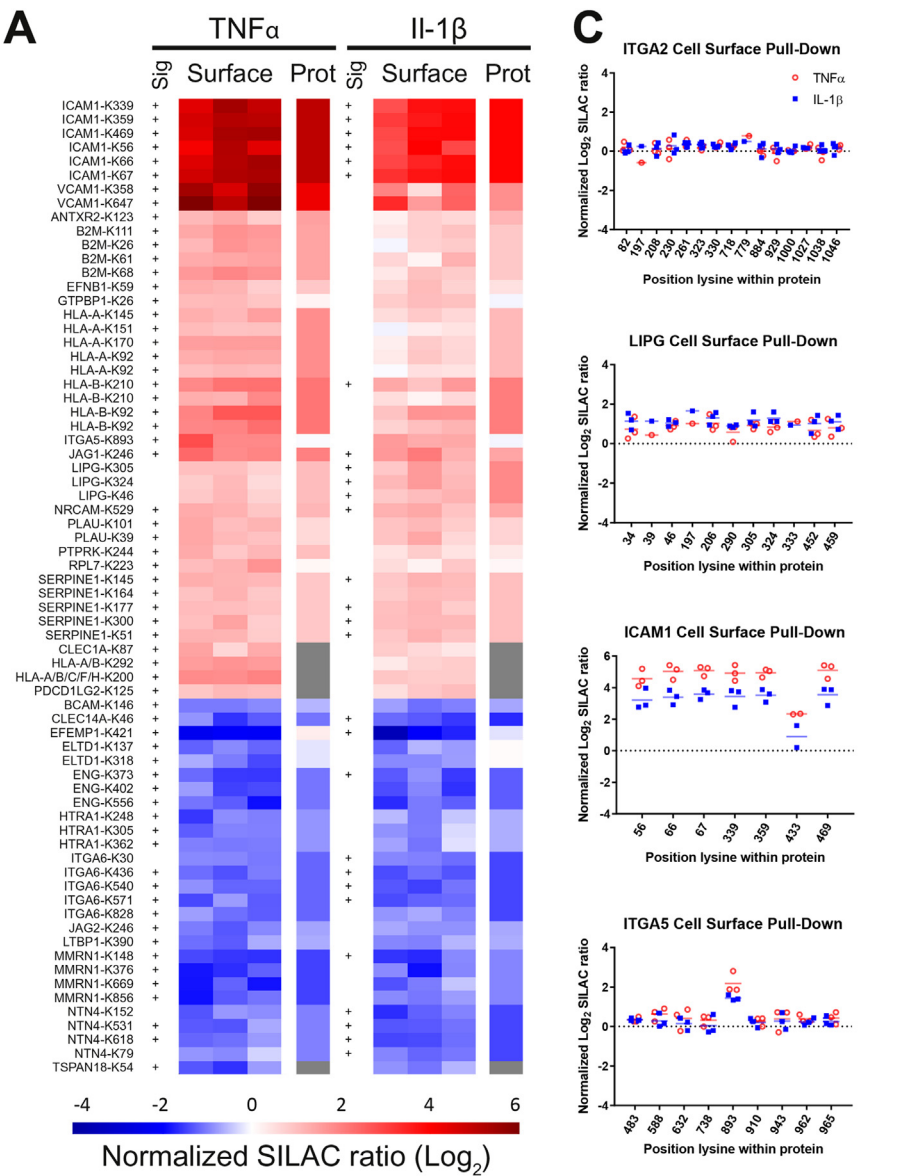
### 3.4. Cytokine-induced inflammation affects the endothelial cell surface

The interaction of ECs with leukocytes and inflammatory mediators is primarily mediated via cell surface proteins. To study proteins specifically localized at the cell surface, we expanded the analysis with quantitative peptide-based cell surface proteomics data. Therefore, ECs, which were cytokine- or mock-treated for 24 h, were incubated with a non-membrane permeable biotin label that chemically modifies lysine residues. After lysis of the cells and enzymatic digestion of the proteins into peptides, biotinylated peptides were pulled-down, and subjected to mass spectrometry analysis. In total, 1260 labeled sites were quantified, representing 359 proteins, of which 70 peptides (originating from 31 proteins) were affected upon cytokine treatment (Fig. 3A, Table S2). A

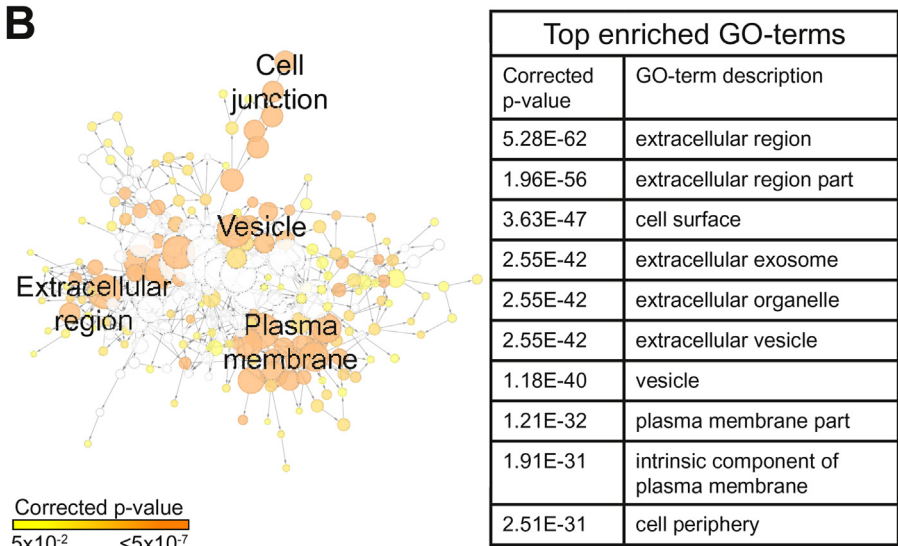
Gene Ontology (GO)-term enrichment analysis was performed in which we compared these 359 proteins to all proteins identified in any of the proteomes. The group of proteins which were biotin-labeled was highly enriched for proteins associated to the extracellular region (Fig. 3B, Table S3), indicating that biotin-labeled peptides originated from the cell surface. In agreement with our proteomic data, TNF $\alpha$  and IL-1 $\beta$  treatment resulted in a highly similar effect on the cell surface proteome, with a slightly stronger response of TNF $\alpha$  for most regulated proteins. These data correlated well with the whole proteomes (Fig. 3A). For most proteins, we identified multiple biotinylated lysine residues, of which the SILAC ratios were consistent throughout the protein (for instance ITGA2 (integrin alpha 2) [non-affected] and LIPG (endothelial lipase) [increased], Fig. 3C). However, our chemical labeling approach also revealed specific changes within proteins, including ITGA5 (integrin alpha 5) position 893 and ICAM1 position 433, although the latter was quantified in only 2 replicates (Fig. 3C). These changes indicate that these sites are more (ITGA5) or less (ICAM1) available for the labeling agent.

### 3.5. Prolonged TNF $\alpha$ -treatment affects protein activation states

Independent of protein expression levels, the activity of proteins can be regulated by post-translational modifications, most notably through phosphorylation [50]. The activation of kinases and phosphatases is a powerful regulatory mechanism to rapidly induce a response, without the need for de novo gene expression and protein production. In order to screen for modified phosphosites after prolonged treatment with TNF $\alpha$ , we assessed the steady-state phosphoproteome by a pull-down approach using Phos-TiO<sub>2</sub> beads. 1728 phosphosites were quantified, which originated from 1045 proteins. Of 67 of these sites, the protein activation state was changed (Fig. 4A and Table S4). The majority of these showed increased phosphorylation levels whereas only about a quarter of the peptides was dephosphorylated (Fig. 4A). For 441 phosphopeptides, originating from 337 proteins, no corresponding whole proteome ratios were available, possibly indicating the low abundance of these proteins. For the remaining phosphosites, the correlation between the whole proteome and the phosphoproteome was poor, in contrast to the cell surface-whole proteome correlation. For a limited number of phosphosites, the phosphosite SILAC ratio reflected the whole proteome SILAC ratio, indicating that the increased phosphorylation reflects increased protein levels (for instance DTX3L [deltex E3 ubiquitin ligase 3L], Fig. 4C). However, for most affected phosphosites, we found no evidence for changes at the protein expression level, suggesting that these phosphosites were regulated by kinase and/or phosphatase activity (e.g. PXN [paxillin], NES [nestin] and AHNAK [neuroblast differentiation-associated protein AHNAK]). For the majority of the phosphorylated proteins, we detected only one or a few regulated phosphosites, suggesting that these may function as on/off switches for function and/or interaction. However, a few proteins appeared to be decorated with differentially regulated phosphosites, indicating that their function may be regulated in a highly complex manner (Fig. 4C: AHNAK and NES). For example, for the scaffold protein AHNAK, we quantified 31 phosphosites in all replicates, of which multiple were regulated, creating a large variety of possibilities to regulate interactions with other proteins. Interestingly, we found one regulated phosphorylation site in ICAM1 at position T530. Although this particular phosphosite was increased compared to control, the



**Fig. 3.** Peptide-based cell surface proteomics allows for quantification of additional cell surface proteins and detects differential labeling within ITGA5. (A) Heat maps of affected cytokine-induced changes of labeled cell surface peptides ('Cell surface') and corresponding median protein values ('Prot'). Color coding represents log<sub>2</sub> SILAC ratios, grey values are not quantified. '+' represents significance. (B) GO term enrichment analysis of labeled proteins compared to all identified proteins. Top 10 enriched GO-terms are depicted in the table. The full analysis is available in Table S-2. (C) Scatter plots of peptides quantified in the cell surface proteome. Values on the X-axis represent the labeled lysine residue in the cell surface proteome. For reference, quantifications present in only 1 or 2 replicates are also depicted in this plot, in contrast other figures and analyses. See also Table S-2 and S-3.



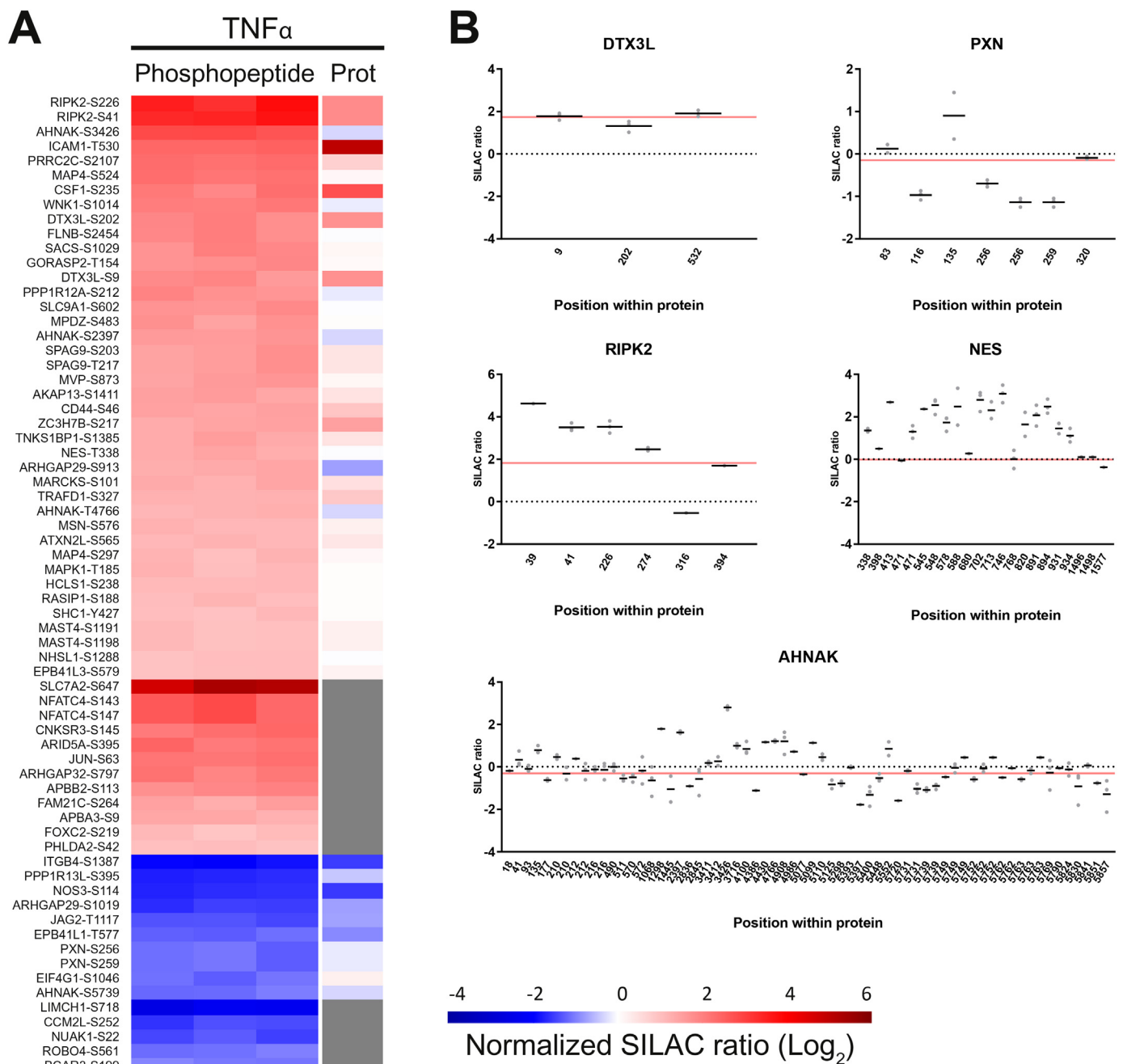


**Fig. 4.** Phosphoproteomic analysis of endothelial inflammation provokes mostly phosphorylation events. (A) Heat map of the quantification of regulated phosphosites. Color coding represents log<sub>2</sub> SILAC ratios. Phosphosites are depicted with corresponding whole proteome SILAC ratios ('Prot'). Grey values are not quantified. (B) SILAC ratios of phosphopeptides (grey dots), lines represent the mean values. Red lines represent median whole proteome values. For reference, modified sites that were not quantified in all replicates have been displayed here as well. See also Table S-4.

protein ratio far exceeded the phosphosite ratio, which indicates that the phosphorylation machinery is not sufficient to modify all available proteins. Alternatively, this could be the result of specific regulation in which the activity of a kinase or phosphatase is affected.

3.6. Integrated analysis of endothelial inflammation

To obtain an overview of all affected processes in endothelial inflammation, we combined data from the whole proteome, cell surface proteome and phosphoproteome and performed a gene ontology (GO)-term enrichment analysis comparing the regulated proteins to all quantified proteins. The enriched GO-terms are partially redundant: a single protein can be present in multiple GO-terms. Based on proteins

shared between GO-terms, the 199 enriched terms were clustered to gain insight in their biological implications (Fig. 5A). Ten subsets were defined and the largest two were visualized as separate networks (Figs. 5B and C). The most prominent GO-terms were related to inflammation, including the immune response and leukocyte migration (Fig. 5A and B). In addition, specific pathways related to increased adhesion molecule expression, self-antigen presentation, cytokine-production and cell migration were enriched as well as generic processes, including signaling, response to stimulus and biological regulation (Table S5). Notably, this analysis emphasizes that many of the affected proteins are part of the extracellular matrix (ECM) or involved in the cell-ECM interaction. Although it has been reported that the ECM plays a role in endothelial inflammation [51], and that TNF $\alpha$  can affect the





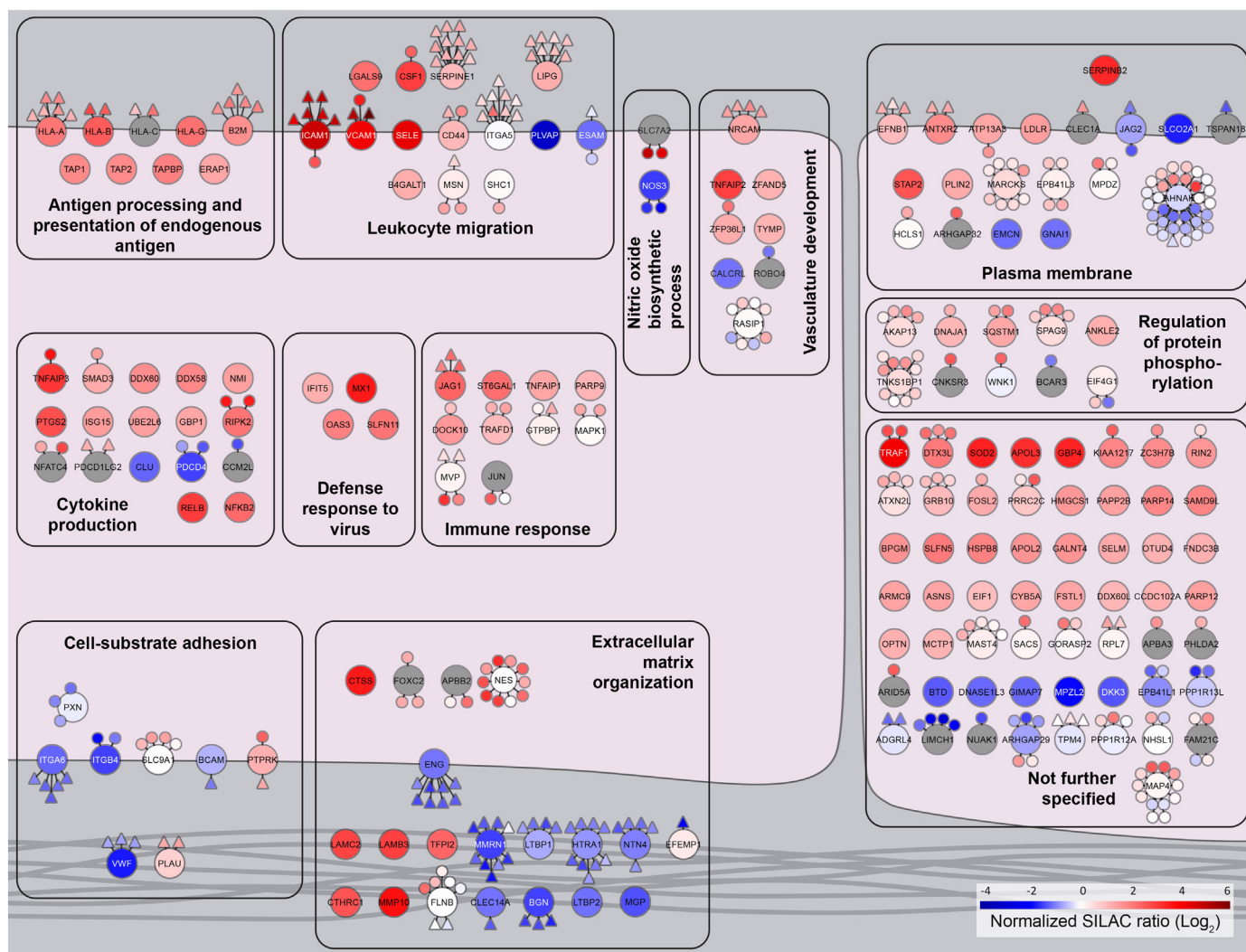


**Fig. 6.** Summary of changed proteins and model of affected processes in TNF $\alpha$ -treated endothelial cells. Schematic overview of affected proteins (large circles), biotin-labels (triangles) and phosphosites (small circles). If a protein is affected in either of the analyses, the protein and all quantified modifications are depicted. The color coding of the proteins and the modifications represent the respective median log<sub>2</sub> SILAC ratios. Non-quantified proteins are depicted grey. Proteins are clustered according to the enrichment analysis of Fig. 5/ Table S-5, with minor manual curation. Localization of proteins within the cell is based on the presence of biotin-modifications and minor manual curation.

important category of proteins which showed an increased expression level relates to endogenous antigen presentation. Expression of the large majority of proteins belonging to peptide-presentation machinery was upregulated after 16 h of TNF $\alpha$  treatment, ranging from the MHC class I complex (B2M [beta-2-microglobulin], HLA [HLA class I histocompatibility antigen]-A/B/C) to peptide transport (TAP [antigen peptide transporter] 1/2, TAPBP [tapasin]) and trimming (ERAP [endoplasmic reticulum aminopeptidase] 1/2). In addition to the endothelium itself, it has been suggested that the ECM also plays a role in endothelial inflammation [51]. In agreement with this hypothesis, we identified regulated expression of a variety of proteins associated with ECM organization. Among the most affected proteins are two laminin subunits:  $\beta$ 3 (LAMB3) and  $\gamma$ 2 (LAMC2), whereas in resting conditions the basement membrane mainly consists of laminin 511 ( $\alpha$ 5 $\beta$ 1 $\gamma$ 1) and 411 [66]. In contrast to these laminins, two laminin receptors (integrin  $\alpha$ 6 $\beta$ 4 [51,67,68] and BCAM [basal cell adhesion molecule]) are decreased, which indicates that the increased laminins do not simply strengthen the cell-ECM interaction. Instead, these may have another function, such as leukocyte interaction, or, after proteolysis, as mediators of inflammation [69]. In addition to proteins that have previously been associated with endothelial inflammation or TNF $\alpha$ , we found

regulated expression of proteins that have remained under the radar so far, including the cell surface proteins ANTXR2 (anthrax toxin receptor 2), EFNB1 (ephrin b1) and CLEC1A (c-type lectin domain family 1 member A).

Endothelial activation is categorized into a rapid transient response (type I activation) and a slower but more sustained response (type II activation) [1]. Type I activation is mediated by (mostly) chemical factors, such as bradykinin, histamine and prostaglandins, that bind to G-protein coupled receptors (GPCRs). GPCRs are typically desensitized within 10–20 min [70], which limits the potential of inflammation and neutrophil extravasation induced by type I activation. In contrast, type II activation is mediated by biochemical factors, such as pro-inflammatory cytokines, binding to their cognate receptors. Since this induces new gene transcription and protein translation, it requires a longer initiation time, however, it also results in a more effective and long-lasting increase in vascular permeability and neutrophil recruitment [1]. Timing of this response in ECs is crucial to prevent excessive leukocyte extravasation and other adverse effects. So far, it has remained unclear how protein expression is regulated over time and if and which feedback mechanisms are in place that shut off inflammatory gene and protein expression. Transcriptomic data from TNF $\alpha$ -treated



fibroblasts indicate a crude classification in 3 kinetic profiles with early, intermediate and late genes, peaking at respectively 0.5, 2 and > 12 h [71] corresponding with the biological processes of leukocyte recruitment, tissue remodeling and wound repair. Our temporal protein data in ECs demonstrate similar profiles, although only two phases can be distinguished. Within the first 4 h a limited number of proteins is synthesized, including the adhesion receptors ICAM1 and SELE. Although protein levels of ICAM1 steadily increase until the 24 h time point, the increase in SELE stops and even decreases, despite continuous presence of the cytokine. This is in agreement with the reported peak of ICAM1 after 48 h [72] and the temporal pattern of SELE expression [16,72,73]. The increased expression of adhesion molecules is followed by a transient decrease in the expression of CTGF and IGFBP7 and a temporal increase in the expression of the 2 subunits of the ferritin complex, FTH1 and FTL. Although TNF $\alpha$  has previously been implicated in the regulation of ferritin levels, albeit only for the heavy and not for the light chain subunit [74], the role of ferritin in TNF $\alpha$ - and IL-1 $\beta$ -treatment of ECs remains unclear. The ferritin complex stores Fe<sup>2+</sup> ions in the non-toxic Fe<sup>3+</sup> form to prevent oxidative damage. It has been described that treatment of ECs with TNF $\alpha$  induces intracellular generation of reactive oxygen species (ROS), a process which requires iron as a catalyst and has been directly associated with destabilization of endothelial junctions [75]. Interestingly, temporal changes in ferritin occur within the same time frame as changes in transendothelial resistance (Fig. 1B), which starts to decrease after 4 h and stabilizes after 8 h. Therefore, we speculate that initially iron is sequestered and utilized to increase ROS production. This results in destabilization of endothelial junctions and degradation of the ferritin complex to replenish available iron levels. Once ROS production is normalized, intracellular iron levels rise and result in ferritin production to levels above the initial concentration, that will eventually normalize. Temporal upregulation of the ferritin complex is followed by a second burst of protein expression, which includes proteins that belong to the self-antigen peptide presentation pathway (HLAs, B2M, ERAP1, TAP1&2 and TAPBP) and proteins involved in conquering viral infections (GBP1 [guanylate binding protein 1], OAS3 [2'-5'-oligoadenylate synthase 3], MX1 and SLFN11 [schlafen family member 11]). Taken together, our results hint towards a two-step process of endothelial inflammation, comprising an initial wave of expression of proteins aimed to attract innate immune cells and mediate their transmigration, followed by a second burst of expression aimed to equip ECs to fight viral infection and present hostile peptides to the immune system, thereby allowing adaptive immune cells to scan the endothelium for possible infections.

The data presented in this study provide novel insight in the effect of TNF $\alpha$ -treatment on ECs, but several questions remain. Our data indicate that TNF $\alpha$  and IL-1 $\beta$  provoke a largely identical response in ECs. Does that imply redundancy, or can more differences be expected in a physiological setting? In vivo, ECs are confronted with many other cytokines, such as IFN- $\gamma$ , which induces MHC class II expression [76], and interleukin 6, which exerts both pro- and anti-inflammatory effects through trans-signaling [77]. Would a combination of any of these cytokines affect additional processes, or evoke a more severe response compared to the individual cytokines? Furthermore, the question remains what the function is of the newly identified cytokine-induced surface proteins. Do these have a role in leukocyte interaction or other processes and why are these processes affected during inflammation? Answers to these questions may further improve our understanding of endothelial inflammation and may eventually aid us in therapeutic intervention of imbalanced inflammation.

Supplementary data to this article can be found online at <https://doi.org/10.1016/j.jprot.2018.08.011>.

#### Author contributions

E.P.B and B.L.v.d.E performed experiments, E.P.B, K.M, A.B.M and M.v.d.B designed the research, E.P.B, A.J.H and B.N analyzed the data

and E.P.B and M.v.d.B wrote the manuscript.

#### Conflict of interest disclosure

The authors have no conflicts of interest to declare.

#### Acknowledgments

The authors would like to thank Dr. Jaap van Buul for his valuable input to improve this manuscript.

#### Funding sources

This work was supported by Sanquin Blood Supply Foundation [grant PPOP 13-002]; and the Landsteiner Foundation for Blood Transfusion Research [LSBR fellowship 1517 to M. van den Biggelaar].

#### References

- [1] J.S. Pober, W.C. Sessa, Evolving functions of endothelial cells in inflammation, *Nat. Rev. Immunol.* 7 (2007) 803–815.
- [2] M.A. Sugimoto, L.P. Sousa, V. Pinho, M. Perretti, M.M. Teixeira, Resolution of inflammation: what controls its onset? *Front. Immunol.* 7 (2016) 160.
- [3] C. Nathan, A. Ding, Nonresolving Inflammation, *Cell* 140 (2010) 871–882.
- [4] R. Medzhitov, Origin and physiological roles of inflammation, *Nature* 454 (2008) 428–435.
- [5] V.W.M. Van Hinsbergh, Endothelium - Role in regulation of coagulation and inflammation, *Semin. Immunopathol.* 34 (2012) 93–106.
- [6] A.H. Sprague, R.A. Khalil, Inflammatory cytokines in vascular dysfunction and vascular disease, *Biochem. Pharmacol.* 78 (2009) 539–552.
- [7] J.S. Pober, M.A.J. Gimbrone, L.A. Lapiere, D.L. Mendrick, W. Fiers, R. Rothlein, T.A. Springer, Overlapping patterns of activation of human endothelial cells by interleukin 1, tumor necrosis factor, and immune interferon, *J. Immunol.* 137 (1986) 1893–1896.
- [8] L. Osborn, C. Hession, R. Tizard, C. Vassallo, S. Lühowskyj, G. Chi-Rosso, R. Lobb, Direct expression cloning of vascular cell adhesion molecule 1, a cytokine-induced endothelial protein that binds to lymphocytes, *Cell* 59 (1989) 1203–1211.
- [9] R. Ciuffa, E. Caron, A. Leitner, F. Uliana, M. Gstaiger, R. Aebersold, Contribution of Mass Spectrometry-based Proteomics to the Understanding of TNF- $\alpha$  Signaling, *J. Proteome Res.* 16 (2017) 14–33.
- [10] D.B. Peterson, T. Sander, S. Kaul, B.T. Wakim, B. Halligan, S. Twigger, K.A. Pritchard, K.T. Oldham, J.S. Ou, Comparative proteomic analysis of PAI-1 and TNF-alpha-derived endothelial microparticles, *Proteomics* 8 (2008) 2430–2446.
- [11] Y. Liu, W. Huang, R. Zhang, J. Wu, L. Li, Y. Tang, Proteomic analysis of TNF- $\alpha$ -activated endothelial cells and endothelial microparticles, *Mol. Med. Rep.* 7 (2013) 318–326.
- [12] G. Sabio, R.J. Davis, TNF and MAP kinase signalling pathways, *Semin. Immunol.* 26 (2014) 237–245.
- [13] J.R. Bradley, J.S. Pober, Tumor necrosis factor receptor-associated factors (TRAFs), *Oncogene* 20 (2001) 6482–6491.
- [14] M.U. Martin, H. Wesche, Summary and comparison of the signaling mechanisms of the Toll/interleukin-1 receptor family, *Biochim. Biophys. Acta - Mol. Cell Res.* 1592 (2002) 265–280.
- [15] J.R. Bradley, TNF-mediated inflammatory disease, *J. Pathol.* 214 (2008) 149–160.
- [16] J.M. Munro, J.S. Pober, R.S. Cotran, Tumor necrosis factor and interferon-gamma induce distinct patterns of endothelial activation and associated leukocyte accumulation in skin of Papio anubis, *Am. J. Pathol.* 135 (1989) 121–133.
- [17] A.G. Kjaergaard, A. Dige, J. Krog, E. Tønnesen, L. Wogensen, Soluble Adhesion Molecules Correlate with Surface Expression in an *In Vitro* Model of Endothelial Activation, *Basic Clin. Pharmacol. Toxicol.* 113 (2013) 273–279.
- [18] J.G. Park, S.Y. Ryu, I.H. Jung, Y.H. Lee, K.J. Kang, M.R. Lee, M.N. Lee, S.K. Son, J.H. Lee, H. Lee, G.T. Oh, K. Moon, H. Shim, Evaluation of VCAM-1 antibodies as therapeutic agent for atherosclerosis in apolipoprotein E-deficient mice, *Atherosclerosis* 226 (2013) 356–363.
- [19] R.L. Brey, A.A. Amato, K. Kagan-Hallet, C.B. Rhine, C.L. Stallworth, Anti-intercellular adhesion molecule-1 (ICAM-1) antibody treatment prevents central and peripheral nervous system disease in autoimmune-prone mice, *Lupus* 6 (1997) 645–651.
- [20] C. Justicia, A. Martín, S. Rojas, M. Gironella, A. Cervera, J. Panés, A. Chamorro, A.M. Planas, Anti-VCAM-1 antibodies did not protect against ischemic damage either in rats or in mice, *J. Cereb. Blood Flow Metab.* 26 (2006) 421–432.
- [21] S. Oguchi, P. Dimayuga, J. Zhu, K.Y. Chyu, J. Yano, P.K. Shah, J. Nilsson, B. Cercek, Monoclonal antibody against vascular cell adhesion molecule-1 inhibits neointimal formation after periaortic carotid artery injury in genetically hypercholesterolemic mice, *Arterioscler. Thromb. Vasc. Biol.* 20 (2000) 1729–1736.
- [22] R.D. Thompson, M.W. Wakelin, K.Y. Larbi, A. Dewar, G. Asimakopoulos, M.A. Horton, M.T. Nakada, S. Nourshargh, Divergent effects of platelet-endothelial cell adhesion molecule-1 and beta 3 integrin blockade on leukocyte transmigration in vivo, *J. Immunol.* 165 (2000) 426–434.
- [23] M.G. Bixel, H. Li, B. Petri, A.G. Khandoga, A. Khandoga, A. Zarbock, K. Wolburg-

- Buchholz, H. Wolburg, L. Sorokin, D. Zeuschner, S. Maerz, S. Butz, F. Krombach, D. Vestweber, CD99 and CD99L2 act at the same site as, but independently of, PECAM-1 during leukocyte diapedesis, *Blood* 116 (2010) 1172–1184.
- [24] V. Makó, J. Czúcz, Z. Weiszhar, E. Herczenik, J. Matkó, Z. Prohászka, L. Cervenak, Proinflammatory activation pattern of human umbilical vein endothelial cells induced by IL-1 $\beta$ , TNF- $\alpha$ , and LPS, *Cytom. Part A* 77 (2010) 962–970.
- [25] J. Martin-Ramirez, M. Hofman, M. van den Biggelaar, R.P. Hebbel, J. Voorberg, Establishment of outgrowth endothelial cells from peripheral blood, *Nat. Protoc.* 7 (2012) 1709–1715.
- [26] M. van den Biggelaar, J.R. Hernández-Fernaudo, B.L. van den Eshof, L.J. Neilson, A.B. Meijer, K. Mertens, S. Zanivan, Quantitative phosphoproteomics unveils temporal dynamics of thrombin signaling in human endothelial cells, *Blood* 123 (2014) e22–e36.
- [27] J.R. Wisniewski, A. Zougman, N. Nagaraj, M. Mann, Universal sample preparation method for proteome analysis, *Nat. Methods* 6 (2009) 359–362.
- [28] J.R. Wisniewski, A. Zougman, M. Mann, Combination of FASP and StageTip-based fractionation allows in-depth analysis of the hippocampal membrane proteome, *J. Proteome Res.* 8 (2009) 5674–5678.
- [29] B.L. van den Eshof, A.J. Hoogendijk, P.J. Simpson, F.P.J. van Alphen, S. Zanivan, K. Mertens, A.B. Meijer, M. van den Biggelaar, Paradigm of Biased PAR1 (Protease-Activated Receptor-1) Activation and Inhibition in Endothelial Cells Dissected by Phosphoproteomics, *Arterioscler. Thromb. Vasc. Biol.* 37 (2017) 1891–1902.
- [30] R.P. Gazendam, A. van de Geer, J.L. van Hamme, A.T.J. Tool, D.J. van Rees, C.E.M. Aarts, M. van den Biggelaar, F. van Alphen, P. Verkuijlen, A.B. Meijer, H. Janssen, D. Roos, T.K. van den Berg, T.W. Kuijpers, Impaired killing of *Candida albicans* by granulocytes mobilized for transfusion purposes: a role for granule components, *Haematologica* 101 (2016) 587–596.
- [31] J. Cox, M. Mann, MaxQuant enables high peptide identification rates, individualized p.P.B.-range mass accuracies and proteome-wide protein quantification, *Nat. Biotechnol.* 26 (2008) 1367–1372.
- [32] M.E. Ritchie, B. Phipson, D. Wu, Y. Hu, C.W. Law, W. Shi, G.K. Smyth, Limma powers differential expression analysis for RNA-sequencing and microarray studies, *Nucleic Acids Res.* 43 (2015) e47.
- [33] J.V. Olsen, B. Blagoev, F. Gnab, D. Macek, C. Kumar, P. Mortensen, M. Mann, Resource global, In Vivo, and Site-Specific Phosphorylation Dynamics in Signaling Networks, vol. 2, 2006, pp. 635–648.
- [34] P. Shannon, A. Markiel, O. Ozier, N.S. Baliga, J.T. Wang, D. Ramage, N. Amin, B. Schwikowski, T. Ideker, Cytoscape: a software Environment for integrated models of biomolecular interaction networks, *Genome Res.* 13 (2003) 2498–2504.
- [35] S. Maere, K. Heymans, M. Kuiper, BiNGO: a Cytoscape plugin to assess over-representation of Gene Ontology categories in Biological Networks, *Bioinformatics* 21 (2005) 3448–3449.
- [36] M.D. Young, M.J. Wakefield, G.K. Smyth, A. Oshlack, Gene ontology analysis for RNA-seq: accounting for selection bias, *Genome Biol.* 11 (2010) R14.
- [37] B. Nota, Gogadget: an R package for interpretation and visualization of GO enrichment results, *Mol. Inform.* 1600132 (2016) 4–7.
- [38] D. Merico, R. Isserlin, O. Stueker, A. Emili, G.D. Bader, Enrichment map: a network-based method for gene-set enrichment visualization and interpretation, *PLoS One* 5 (2010) e13984.
- [39] L.M. Raaijmakers, P. Giansanti, P.A. Possik, J. Mueller, D.S. Peeper, A.J.R. Heck, A.F.M. Altaalar, PhosphoPath: visualization of phosphosite-centric dynamics in temporal molecular networks, *J. Proteome Res.* 14 (2015) 4332–4341.
- [40] J.A. Vizcaino, E.W. Deutsch, R. Wang, A. Csordas, F. Reisinger, D. Rios, J.A. Dianas, Z. Sun, T. Farrah, N. Bandeira, P.A. Binz, I. Xenarios, M. Eisenacher, G. Mayer, L. Gatto, A. Campos, R.J. Chalkley, H.J. Kraus, J.P. Albar, S. Martinez-Bartolomé, R. Apweiler, G.S. Omenn, L. Martens, A.R. Jones, H. Hermjakob, ProteomeXchange provides globally coordinated proteomics data submission and dissemination, *Nat. Biotechnol.* 32 (2014) 223–226.
- [41] J. Brett, H. Gerlach, P. Nawroth, S. Steinberg, G. Godman, D. Stern, Tumor necrosis factor/cachectin increases permeability of endothelial cell monolayers by a mechanism involving regulatory G proteins, *J. Exp. Med.* 169 (1989) 1977–1991.
- [42] J.T.B. Crawley, S. Zanardelli, C.K.N.K. Chion, D.A. Lane, The central role of thrombin in hemostasis, *J. Thromb. Haemost.* 5 (2007) 95–101.
- [43] B. Franzén, K. Duvefelt, C. Jonsson, B. Engelhardt, J. Ottervald, M. Wickman, Y. Yang, I. Schuppe-Koistinen, Gene and protein expression profiling of human cerebral endothelial cells activated with tumor necrosis factor- $\alpha$ , *Brain Res. Mol. Brain Res.* 115 (2003) 130–146.
- [44] M. Rothe, S.C. Wong, W.J. Henzel, D.V. Goeddel, A novel family of putative signal transducers associated with the cytoplasmic domain of the 75 kDa tumor necrosis factor receptor, *Cell* 78 (1994) 681–692.
- [45] D. Venkatesh, T. Hernandez, F. Rosetti, I. Batal, X. Cullere, F.W. Luscinskas, Y. Zhang, G. Stavrakis, G. García-Cardena, B.H. Horwitz, T.N. Mayadas, Endothelial TNF Receptor 2 Induces IRF1 Transcription Factor-Dependent Interferon- $\beta$  Autocrine Signaling to Promote Monocyte Recruitment, *Immunity* 38 (2013) 1025–1037.
- [46] M. Yoshizumi, M.A. Perrella, J.C. Burnett, M.E. Lee, Tumor necrosis factor down-regulates an endothelial nitric oxide synthase mRNA by shortening its half-life, *Circ. Res.* 73 (1993) 205–209.
- [47] A. Bernardo, C. Ball, L. Nolasco, J.F. Moake, J.F. Dong, Effects of inflammatory cytokines on the release and cleavage of the endothelial cell-derived ultralarge von Willebrand-factor multimers under flow, *Blood* 104 (2004) 100–106.
- [48] P. Rantakari, K. Auvinen, N. Jäppinen, M. Kapraali, J. Valtonen, M. Karikoski, H. Gerke, I. Iftakhar-E-Khuda, J. Keuschnigg, E. Umemoto, K. Tohya, M. Miyasaka, K. Elima, S. Jalkanen, M. Salmi, The endothelial protein PLVAP in lymphatics controls the entry of lymphocytes and antigens into lymph nodes, *Nat. Immunol.* 16 (2015) 386–396.
- [49] R.V. Stan, D. Tse, S.J. Deharvengt, N.C. Smits, Y. Xu, M.R. Luciano, C.L. McGarry, M. Buitendijk, K.V. Nemani, R. Elgueta, T. Kobayashi, S.L. Shipman, K.L. Moodie, C.P. Daghighian, P.A. Ernst, H.K. Lee, A.A. Suriawinata, A.R. Schmed, D.S. Longnecker, S.N. Fiering, R.J. Noelle, B. Gimí, N.W. Shworak, C. Carrière, The diaphragms of fenestrated endothelia: gatekeepers of vascular permeability and blood composition, *Dev. Cell* 23 (2012) 1203–1218.
- [50] G.A. Khoury, R.C. Baliban, C.A. Floudas, Proteome-wide post-translational modification statistics: frequency analysis and curation of the swiss-prot database, *Sci. Rep.* 1 (2011) 90.
- [51] L. Sorokin, The impact of the extracellular matrix on inflammation, *Nat. Rev. Immunol.* 10 (2010) 712–723.
- [52] M. Sixt, B. Engelhardt, F. Pausch, R. Hallmann, O. Wendler, L.M. Sorokin, Endothelial cell laminin isoforms, laminins 8 and 10, play decisive roles in T cell recruitment across the blood-brain barrier in experimental autoimmune encephalomyelitis, *J. Cell Biol.* 153 (2001) 933–946.
- [53] M. Frieser, H. Nöckel, F. Pausch, C. Röder, A. Hahn, R. Deutzmann, L.M. Sorokin, Cloning of the mouse laminin  $\alpha 4$  cDNA. Expression in a subset of endothelium, *Eur. J. Biochem.* 246 (1997) 727–735.
- [54] P.R. Karhemo, S. Ravela, M. Laakso, I. Ritamo, O. Tatti, S. Mäkinen, S. Goodison, U.H. Stenman, E. Hölttä, S. Hautaniemi, L. Valmu, K. Lehti, P. Laakkonen, An optimized isolation of biotinylated cell surface proteins reveals novel players in cancer metastasis, *J. Proteome Res.* 11 (2012) 87–100.
- [55] K. Hörmann, A. Stukalov, A.C. Müller, L.X. Heinz, G. Superti-Furga, J. Colinge, K.L. Bennett, A Surface biotinylation strategy for reproducible plasma membrane protein purification and tracking of genetic and drug-induced alterations, *J. Proteome Res.* 15 (2016) 647–658.
- [56] W.Y. Sun, S.M. Pitson, C.S. Bonder, Tumor necrosis factor-induced neutrophil adhesion occurs via sphingosine kinase-1-dependent activation of endothelial  $\alpha 5 \beta 1$  integrin, *Am. J. Pathol.* 177 (2010) 436–446.
- [57] P.L. Reilly, J.R. Woska, D.D. Jeanfavre, E. McNally, R. Rothlein, B.J. Bormann, The native structure of intercellular adhesion molecule-1 (ICAM-1) is a dimer. Correlation with binding to LFA-1, *J. Immunol.* 155 (1995) 529–532.
- [58] Y. Yang, C.D. Jun, J.H. Liu, R. Zhang, A. Joachimiak, T.A. Springer, J.H. Wang, Structural basis for dimerization of ICAM-1 on the cell surface, *Mol. Cell* 14 (2004) 269–276.
- [59] J. Miller, R. Knorr, M. Ferrone, R. Houdei, C.P. Carron, M.L. Dustin, Intercellular adhesion molecule-1 dimerization and its consequences for adhesion mediated by lymphocyte function associated-1, *J. Exp. Med.* 182 (1995) 1231–1241.
- [60] R. Martinelli, G. Newton, C.V. Carman, J. Greenwood, F.W. Luscinskas, Novel role of CD47 in rat microvascular endothelium: Signaling and regulation of T-cell transendothelial migration, *Arterioscler. Thromb. Vasc. Biol.* 33 (2013) 2566–2576.
- [61] Y. Kojima, K.I. Hirata, T. Ishida, Y. Shimokawa, N. Inoue, S. Kawashima, T. Quertermous, M. Yokoyama, Endothelial lipase modulates monocyte adhesion to the vessel wall: a potential role in inflammation, *J. Biol. Chem.* 279 (2004) 54032–54038.
- [62] L. Chi, Y. Li, L. Stehno-Bittel, J. Gao, D.C. Morrison, D.J. Stechschulte, K.N. Dileepan, Interleukin-6 production by endothelial cells via stimulation of protease-activated receptors is amplified by endotoxin and tumor necrosis factor- $\alpha$ , *J. Interf. Cytokine Res.* 21 (2001) 231–240.
- [63] V.I. Otto, U.E. Heinzel-Plaines, S.M. Gloor, O. Trentz, T. Kossmann, M.C. Morganti-Kossmann, sICAM-1 and TNF- $\alpha$  induce MIP-2 with distinct kinetics in astrocytes and brain microvascular endothelial cells, *J. Neurosci. Res.* 60 (2000) 733–742.
- [64] K. Kinoshita, K. Tanjoh, A. Noda, A. Sakurai, J. Yamaguchi, T. Azuhata, A. Utagawa, T. Moriya, Interleukin-8 production from Human Umbilical Vein Endothelial Cells during Brief Hyperglycemia: the effect of Tumor Necrotic Factor- $\alpha$ , *J. Surg. Res.* 144 (2008) 127–131.
- [65] R. Sala, B.M. Rotoli, E. Colla, R. Visigalli, A. Parolari, O. Bussolati, G.C. Gazzola, V. Dall'Asta, Two-way arginine transport in human endothelial cells: TNF- $\alpha$  stimulation is restricted to system y(+), *Am. J. Physiol. Cell Physiol.* 282 (2002) C134–C143.
- [66] J. Di Russo, M.-J. Hannocks, A.-L. Luik, J. Song, X. Zhang, L. Yousif, G. Aspite, R. Hallmann, L. Sorokin, Vascular laminins in physiology and pathology, *Matrix Biol.* 57–58 (2016) 140–148.
- [67] A.G. Arroyo, M.L. Iruela-Arispe, Extracellular matrix, inflammation, and the angiogenic response, *Cardiovasc. Res.* 86 (2010) 226–235.
- [68] R. Laug, M. Fehrholz, N. Schütze, B.W. Kramer, V. Krump-Konvalinkova, C.P. Speer, S. Kunzmann, IFN- $\gamma$  and TNF- $\alpha$  synergize to inhibit CTGF expression in human lung endothelial cells, *PLoS One* 7 (2012) 1–10.
- [69] T.L. Adair-Kirk, R.M. Senior, Fragments of extracellular matrix as mediators of inflammation, *Int. J. Biochem. Cell Biol.* 40 (2008) 1101–1110.
- [70] R.R. Gainetdinov, R.T. Premont, L.M. Bohn, R.J. Lefkowitz, M.G. Caron, Desensitization of G protein-coupled receptors and neuronal functions, *Annu. Rev. Neurosci.* 27 (2004) 107–144.
- [71] S. Hao, D. Baltimore, The stability of mRNA influences the temporal order of the induction of genes encoding inflammatory molecules, *Nat. Immunol.* 10 (2009) 281–288.
- [72] S.J. O'Carroll, D.T. Kho, R. Wiltshire, V. Nelson, O. Rotimi, R. Johnson, C.E. Angel, E.S. Graham, Pro-inflammatory TNF $\alpha$  and IL-1 $\beta$  differentially regulate the inflammatory phenotype of brain microvascular endothelial cells, *J. Neuroinflammation* 12 (2015) 131.
- [73] J.S. Pober, M.P. Bevilacqua, D.L. Mendrick, L.A. Lapierre, W. Fiers, M.A. Gimbrone, Two distinct monokines, interleukin 1 and tumor necrosis factor, each independently induce biosynthesis and transient expression of the same antigen on the surface of cultured human vascular endothelial cells, *J. Immunol.* 136 (1986) 1680–1687.
- [74] S.V. Torti, E.L. Kwak, S.C. Miller, L.L. Miller, G.M. Ringold, K.B. Myambo, A.P. Young, F.M. Torti, The molecular cloning and characterization of murine



- ferritin heavy chain, a tumor necrosis factor-inducible gene, *J. Biol. Chem.* 263 (1988) 12638–12644.
- [75] B. Marcos-Ramiro, D. García-Weber, J. Millán, TNF-induced endothelial barrier disruption: beyond actin and Rho, *Thromb. Haemost.* 112 (2014) 1088–1102.
- [76] T. Collins, A.J. Korman, C.T. Wake, J.M. Boss, D.J. Kappes, W. Fiers, K.A. Ault, M.A. Gimbrone, J.L. Strominger, J.S. Pober, Immune interferon activates multiple class II major histocompatibility complex genes and the associated invariant chain gene in human endothelial cells and dermal fibroblasts, *Proc. Natl. Acad. Sci. U. S. A.* 81 (1984) 4917–4921.
- [77] J. Scheller, A. Chalaris, D. Schmidt-Arras, S. Rose-John, The pro- and anti-inflammatory properties of the cytokine interleukin-6, *Biochim. Biophys. Acta* 1813 (2011) 878–888.